CRYSTAL GROWTH & DESIGN

pubs.acs.org/crystal

Article

Methyl Groups as Hydrogen Bond Acceptors via Their sp^3 Carbon Atoms

Published as part of a Crystal Growth and Design virtual special issue on Emerging Investigators 2022

Oliver Loveday and Jorge Echeverría*

Cite This: *Cryst. Growth Des.* 2021, 21, 5961−5966

Read Online

ACCESS | Metrics & More | Article Recommendations | Supporting Information

ABSTRACT: We report herein a combined structural and theoretical study of a novel hydrogen bond in which a methyl group, when bound to an electropositive atom E, acts as the acceptor via its carbon atom. A significant number of experimental examples of such interactions have been retrieved from the Cambridge Structural Database, showing a clear trend toward a linear arrangement of the two interacting groups (E−CH_3···H−Y) as the interatomic distance shortens. The hydrogen bond has been further investigated by means of different computational techniques in order to assess its strength and nature. We have also unveiled, by means of natural bond orbital analysis, a charge transfer from a σ(E−C) bonding orbital of the methyl group to a σ^* antibonding H−Y orbital.

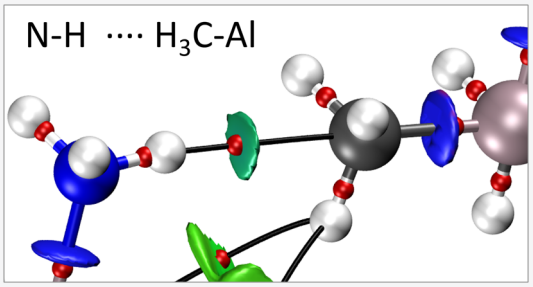

INTRODUCTION

The hydrogen bond plays a key role in many chemical and biological processes. It is established between a protic hydrogen atom bound to an electronegative atom (the H-bond donor) and an electron-rich species (the H-bond acceptor). In most cases, the H-bond acceptor contains a lone pair, but it has been seen that this role can be played by other electron-rich systems such as a π-bond,[1,2] a radical,[3] or even a σ-bond.[4]

If we narrow our focus on carbon, this element usually participates in H-bonding with sp^2 and sp hybridization, donating electron density through C═C and C≡C bonds.[2,5,6] On the other hand, sp^3 carbon atoms show an electron density depletion when connected to more electronegative atoms, which is the origin of tetrel bonding.[7−9] Conversely, if the carbon atom is bound to a less electronegative atom, the electron density is displaced toward the former, and the charge distribution can be disclosed by mapping the molecular electrostatic potential (MEP). Consequently, electron-rich sp^3-C atoms have been observed to participate in some types of noncovalent interactions as electron density donors.[10]

If the sp^3-C atom is bound to H or another C atom, the MEP at the former is slightly negative but very close to zero.[10] This small accumulation of electron density might be enough for the carbon atom to act as a weak electron density donor. Early theoretical work on the potential energy surface of the methane−water complex was reported by Cieplak et al.[11] This system was then widely studied by means of computational techniques. The work by Isaev, who comprehensively characterized the O−H···C hydrogen bond in the aforementioned methane−water complex,[12,13] deserves special mention. In 2009, Olesen and Hammerum reported a hydrogen bond between protonated water and the C−H σ-bonds in small alkanes.[14] X−H···C hydrogen bonds between HF and linear alkanes were identified and characterized by Parajuli and Arunan showing that they are stronger than C−H···X ones.[15]

We present herein structural and computational evidence for the existence of a novel type of hydrogen bond in which the acceptor is a sp^3 carbon atom of a methyl group which is connected to an atom less electronegative than carbon, e.g. B, Al or Si. The substitution of one of the H atoms in methane with an electropositive atom increases the electron density at the C atom, making it in this way more prone to behave as a H-bond acceptor. We have demonstrated that this unexplored hydrogen bond is found in many crystal structures, and it exhibits precise geometrical arrangements. Furthermore, its nature and strength have been characterized by means of several computational tools.

RESULTS AND DISCUSSION

To try to get a general picture of the occurrence and geometries associated with hydrogen bonds in which a methyl group acts at the acceptor, the Cambridge Structural Database (CSD)[16] has been explored. We have searched for short E−

Received: July 28, 2021
Published: September 13, 2021

https://doi.org/10.1021/acs.cgd.1c00853
Cryst. Growth Des. 2021, 21, 5961−5966

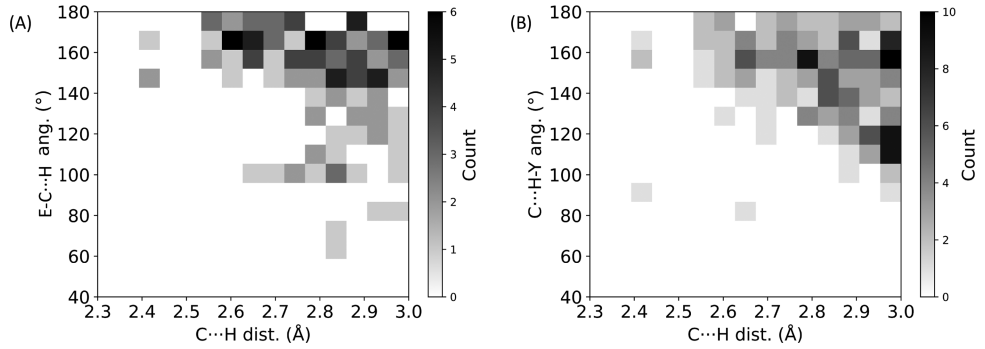

Figure 1. Characteristic (A) E−C···H (E = B, Al, Ga, In, Tl, Si, Ge, Sn, Pb) and (B) C···H−Y angles as a function of the interatomic C···H distance for methyl···H−Y (Y = N, O, S, Se) contacts shorter than the sum of the van der Waals radii (2.97 Å) as found in the CSD.

CH_3···H−Y (E = B, Al, Ga, In, Tl, Si, Ge, Sn, Pb; Y = N, O, S, Se) contacts, limited to C···H distances shorter than the sum of the van der Waals radii (2.97 Å).[17] We have found a total of 136 structures containing intermolecular C···H short contacts. In 114 of them, the H atom involved in the C···H contact shows no further contacts with other atoms at distances shorter than the sum of the vdW radii. Within this set of structures, it is likely that the short contact between the methyl group and the protic hydrogen atom is not supported by any other directional interaction.

Some geometrical trends appear if we look in detail at the angles associated with short contacts within the aforementioned structural set (Figure 1). Remarkably, both the E−C···H (Figure 1A) and C···H−Y (Figure 1B) angles tend to 180° as the C···H distance shortens, which is consistent with the existence of a hydrogen bond-like interaction. Such behavior has been previously observed in similar interactions, and it is characteristic of significantly directional interactions.[18−21]

On the other hand, there are 146 structures with dihydrogen H···H contacts shorter than the van der Waals radii sum (2.40 Å). Among the latter, in 85 structures the H···H short distance is the result of a C···H contact at the same methyl group. In the other 61 structures, there is no C···H contact accompanying the H···H one, but, in most cases, the latter is the consequence of an O···H (e.g., VOTTOP,[22] FENYAY[23]) or N···H (e.g., MICCUZ,[24] MOZWAZ[25]) hydrogen bond. Thus, it is possible that, due to the chemical composition of the interacting groups, stabilizing dihydrogen interactions[26−28] may appear accompanying the C···H hydrogen bonds.

To try to understand a possible electrostatic origin of the studied interactions, we have represented the molecular electrostatic potential (MEP) of $(CH_3)_3Al$-NH_3 (Figure 2). This is a simple molecule that contains the two interacting moieties, namely, Al-CH_3 and NH, and that has been seen to establish an Al-CH_3···H−N short contact (2.73 Å) in its crystal structure (LINZOX).[29] The MEP map shows two clearly differentiated regions of positive and negative charge, corresponding to the NH_3 and CH_3 groups, respectively. In the NH_3 region, the most positive MEP value ($V_{s,max}$ = +56.3 kcal/mol) is associated with the three hydrogen atoms. On the other hand, in the methyl groups, the most negative point of the electrostatic potential is located at the center of the plane formed by the three hydrogen atoms ($V_{s,min}$ = −21.5 kcal/mol). The asymmetry in the MEP distribution is due to the presence of the ammonia group that induces some charge depletion in the region of the methyl group that is closest to the ammonia. It has been previously observed that, in the molecule of trimethyl-aluminum, the MEP map of the methyl

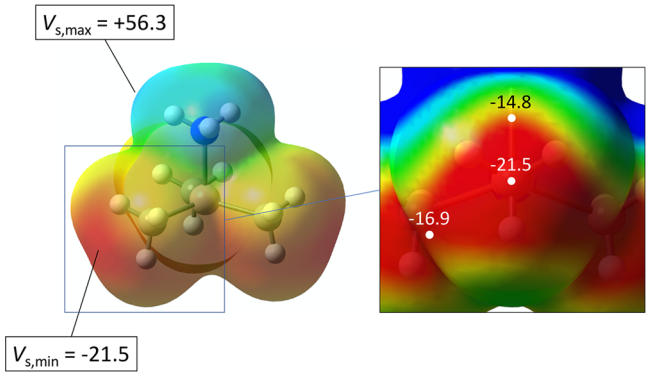

Figure 2. Molecular electrostatic potential map (s = 0.001 au) of $(CH_3)_3Al$-NH_3 (LINZOX). Electrostatic potential values are given in kcal/mol.

groups shows a 3-fold symmetry with the most negative point still at the center of the three hydrogen atoms.[10] Therefore, the MEP map in Figure 2 clearly predicts an electrostatically favored interaction between the N−H and CH_3 moieties, more specifically with the carbon atom of the latter. This is in very good agreement with the results of the above structural analysis, in which the shorter the C···H distance, the more linear the E−C···H−Y framework (Figure 1).

Next, we have selected four experimental examples of interacting dimers featuring E-CH_3···HN interactions for E = B, Al, Ga, and Si (BUFWUV,[30] LINZOX, LUVYOQ,[31] and JESLOI,[32] respectively; Figure 3). All dimers show H···C distances shorter than the sum of the vdW radii, and the E−C···H−N framework is close to linearity in all cases. The corresponding interaction energies have been calculated at the DLPNO-CCSD(T) level on the crystallographic coordinates with the positions of all H atoms optimized at the M06-2X/def2-TZVPD (Table 1). Interaction energies are in the range −3.01 to −5.78 kcal/mol, but it is hard to say which part of those energies is due to the CH_3···H−N interaction. A previous theoretical report estimated at −0.9 kcal/mol the interaction energy of the C···H bond in the methane−water adduct.[12]

We have chosen this computational approach to try to mimic the scenario found in the solid state. However, the interaction energies have been also computed both on the fully optimized dimers and on the crystallographic coordinates without further optimization (see complete results in the Supporting Information; Table S1). In general, the strength of the interaction increases from the nonoptimized systems to the

https://doi.org/10.1021/acs.cgd.1c00853
Cryst. Growth Des. 2021, 21, 5961−5966

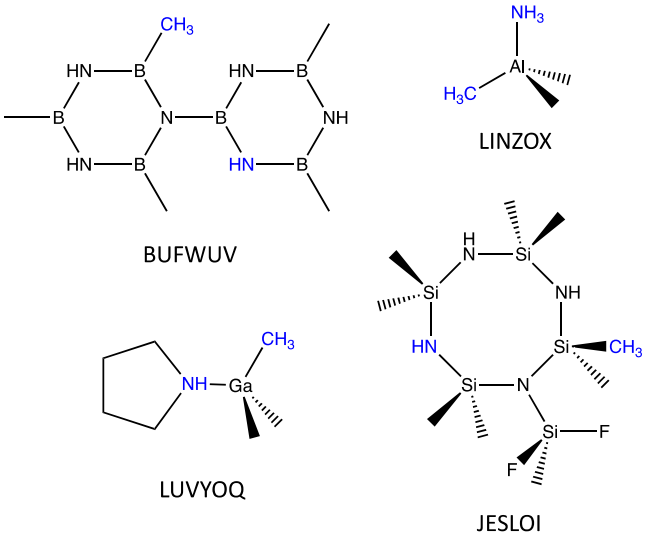

Figure 3. Chemical structures, with the corresponding CSD refcodes, of the four molecules studied here that are involved in $-CH_3\cdots HN$ hydrogen bonds, with the two interacting groups highlighted in blue.

Table 1. Main Geometrical Parameters and BSSE-Corrected Interaction Energies Calculated at the M06-2X//DLPNO-CCSD(T) Level of Theory with the def2-TZVPD Basis Set for All Atoms for the Dimers under Study[a]

refcode	$d_{C\cdots H}$ (Å)	E−C···H ang. (deg)	C···H−N ang. (deg)	ΔE_{int} (kcal/mol)
BUFWUV	2.52	177.7	177.8	−3.01
LINZOX	2.61	179.5	171.3	−3.45
LUVYOQ	2.47	177.3	176.8	−4.15
JESLOI	2.69	174.8	165.6	−5.78

[a]Only the H atoms involved in the $CH_3\cdots HN$ interaction were optimized from the crystallographic coordinates.

H-optimized ones, and it is maximum in the fully optimized dimers. For the latter, the intermolecular distances significantly shorten upon geometry optimization, keeping the linearity of the E−C···H−N moieties (see structures in the Supporting Information). Furthermore, in the fully optimized dimers LINZOX and LUVYOQ, there is an increase of the N−H bond length in the interacting unit with respect to the noninteracting N−H groups of around 0.003−0.005 Å. Similarly, an increase in the interacting Al−C and Ga−C bonds lengths in LINZOX and LUVYOQ is also observed (+0.015 and +0.020 Å, respectively).

The topology of the electron density of the four dimers has also been studied by means of the Quantum Theory of Atoms in Molecules (QTAIM)[33] and the noncovalent interaction index (NCI).[34] The results are presented in Figure 4. Remarkably, in all cases there is a bond path between the carbon and hydrogen atoms involved in the interaction. The values of the electron density and its Laplacian at the bond critical points are within the expected range for weakly hydrogen-bonded neutral molecules (see complete results in the Supporting Information).[35] Moreover, the associated NCI isosurfaces show a disk-like shape which is characteristic of hydrogen bonds. The shape of the isosurfaces in the dimers with the shortest C···H contacts, namely, BUFVUW and LUVYOQ, is more triangular because the three N−H···H−C distances are within the sum of the vdW radii (2.40 Å). Note that in the case of LUVYOQ, the color of the NCI isosurface is

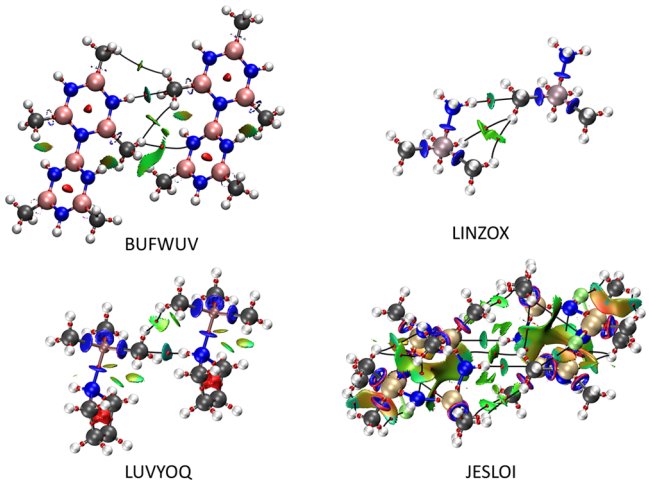

Figure 4. QTAIM+NCI plots of the four dimers under study calculated at the M06-2X/def2-TZVPD level of theory. BCPs and BPs are represented as red spheres and black lines, respectively. Blue, green, and red NCI isosurfaces are associated with strong covalent, weak attractive, and repulsive interactions, respectively.

bluer, indicating a stronger interaction. Other bond paths between the monomers are associated with ubiquitous dihydrogen interactions, which undoubtedly contribute to the overall stability of the dimers.[26−28]

The electron density shift (EDS) is a very useful tool to visualize the changes in the electron density in two isolated molecules upon complexation, and it has been widely applied to the study of noncovalent interactions.[36−39] We have calculated the EDS maps of the four analyzed dimers, and the results are depicted in Figure 5. It can be observed that, in

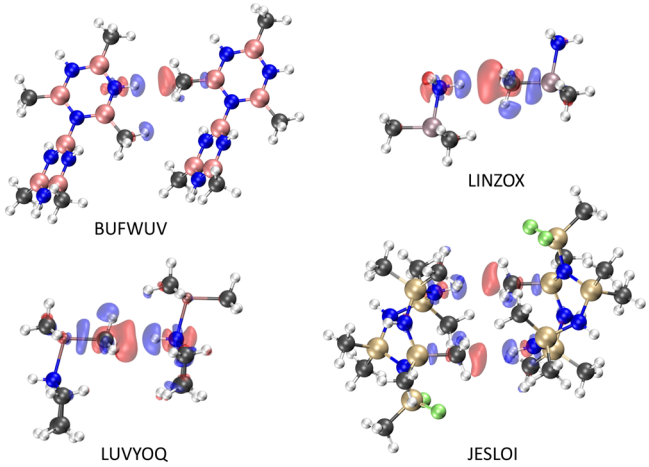

Figure 5. Electron density shift (EDS) maps for the four dimers under study represented at the 0.0005 au isovalue calculated at the M06-2X/def2-TZVPD level of theory. Blue and red represent negative and positive values of the EDS, respectively.

all cases, there is an increase in the electron density at the extension of the E−C bond of the interacting methyl group (red regions). On the other hand, the H-bond donor, i.e., the hydrogen atom, shows a blue region that indicates a decrease of the electron density. These pictures are very similar to those found in previous EDS studies of hydrogen bonds, both intra-[40] and intermolecular.[41,42]

https://doi.org/10.1021/acs.cgd.1c00853
Cryst. Growth Des. 2021, 21, 5961−5966

Natural bond orbital (NBO) analyses have been carried out to disclose the dominant orbital interactions involved in the studied hydrogen bonds. Second-order perturbation energies for the different charge transfer processes in the four dimers under study are summarized in Figure 6. In all cases, the most

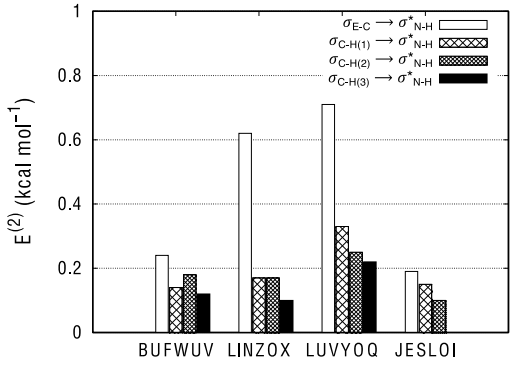

Figure 6. Second-order perturbation energies $E^{(2)}$ for relevant charge transfer processes in the four dimers under study obtained by means of an NBO analysis.

important orbital interaction is a charge transfer from a σ occupied E−C orbital into an empty σ^* antibonding N−H orbital. Such interactions are particularly relevant in LINZOX and LUVYOQ, accounting for 0.62 and 0.71 kcal/mol, respectively. On the other hand, we also found charge transfer processes from the three σ(C−H) bonding orbitals of the methyl group into the same empty σ^* antibonding N−H orbital. These interactions are less energetic than the σ(E−C) → σ^*(N−H) one, with second-order perturbation energies ranging from 0.10 to 0.33 kcal/mol. In JESLOI, only two σ(C−H) orbitals are found to act as donors probably due to the lower value of the C···H−N angle that separates the third σ(C−H) orbital from the interacting region. The NBO results are consistent with the hypothesis of the interaction as a hydrogen bond, although in this case there is no lone pair acting as electron density donor but a σ-bonding orbital of a methyl group.

CONCLUSIONS

We have reported herein a novel hydrogen bond between a protic hydrogen atom and the sp^3-C atom of a methyl group, acting as the hydrogen bond donor and acceptor, respectively. To accumulate the electron density in the C atom, the methyl group must be bound to an atom E that is less electronegative than carbon (e.g., E = B, Al, Si). This hydrogen bond can be extensively found in the solid state showing a high degree of linearity, especially for short C···H distances. MEP, QTAIM, NCI, and EDS calculations helped us to demonstrate that the interaction occurs mainly via the methyl carbon atom with contributions of the hydrogen atoms. NBO analyses showed that the sp^3 carbon atom, despite not having available lone pairs, is able to donate electron density from a σ(E−C) bonding orbital. These results allow new uses of sp^3−C atoms in crystal design and open the possibility of exploring other scenarios in which methyl groups can behave as electron density donors.

COMPUTATIONAL DETAILS

Structural searches were carried out in the Cambridge Structural Database (CSD), version 5.41 (November 2019) with three updates.[16] We only considered crystal structures with 3D coordinates defined, nondisordered, with no errors, not polymeric and with R lower than 0.05. CSD identifiers are given throughout the manuscript as six-letter refcodes (e.g., ABCDEF). The van der Waals radii proposed by Alvarez were used.[17]

DFT calculations were performed with the M06-2X functional and the def2-TZVPD basis sets for all atoms. We chose the M06-2X functional because it has shown very good performance with noncovalent interactions in previous benchmark reports.[43,44] Dimers were analyzed in three different geometries: the crystallographic coordinates, the crystallographic coordinates with the H atoms optimized, and the fully optimized coordinates. All geometry, both partial and total, were done at the M06-2X/def2-TZVPD level. Interaction energies were calculated via the supermolecule approach and corrected for the BSSE by means of the counterpoise method.[45] DLPNO-CCSD(T) calculations were done on the DFT geometries with the ORCA 4.2.1 software.[46] DFT and MP2 calculations were carried out with Gaussian16.[47]

MEP maps were built on the 0.001 Å electron density isosurface with GaussView.[48] QTAIM and NCI topological analyses of the electron density were carried out with MultiWfn 3.7 on the DFT wave function.[49] NBO analysis was done with the NBO3.1 software[50] as implemented in Gaussian16 at the DFT level. EDS surfaces ($EDS_{AB} = \rho(AB) - \rho(A) - \rho(B)$) were generated with MultiWfn 3.7 and represented with VMD 1.9.3.[51]

ASSOCIATED CONTENT

Supporting Information

The Supporting Information is available free of charge at https://pubs.acs.org/doi/10.1021/acs.cgd.1c00853.

Interaction energies at the DFT, MP2, and DLPNO-CCSD(T) levels, complete NBO results, detailed QTAIM analysis, full list of CSD refcodes and Cartesian coordinates of partially and fully optimized systems (PDF)

AUTHOR INFORMATION

Corresponding Author

Jorge Echeverría − *Departament de Química Inorgànica i Orgànica, Universitat de Barcelona, 08028 Barcelona, Spain; Institut de Química Teòrica i Computacional IQTC-UB, 08028 Barcelona, Spain;* orcid.org/0000-0002-8571-0372; Email: jorge.echeverria@qi.ub.es

Author

Oliver Loveday − *Departament de Química Inorgànica i Orgànica, Universitat de Barcelona, 08028 Barcelona, Spain*

Complete contact information is available at: https://pubs.acs.org/10.1021/acs.cgd.1c00853

Notes

The authors declare no competing financial interest.

ACKNOWLEDGMENTS

J.E. is grateful to the Spanish MICCIN for a Ramón y Cajal research contract (RYC-2017-22853). Financial support from the Spanish Structures of Excellence María de Maeztu program (MDM-2017-0767) and Spanish MICINN through Grant PID2019-109119GA-I00 is gratefully acknowledged.

REFERENCES

(1) Suezawa, H.; Yoshida, T.; Umezawa, Y.; Tsuboyama, S.; Nishio, M. CH/π interactions implicated in the crystal structure of transition metal compounds - A database study. *Eur. J. Inorg. Chem.* **2002**, *2002*, 3148−3155.

(2) Nishio, M. CH/π hydrogen bonds in crystals. *CrystEngComm* **2004**, *6*, 130−158.

(3) Hammerum, S. Alkyl Radicals as Hydrogen Bond Acceptors: Computational Evidence. *J. Am. Chem. Soc.* **2009**, *131*, 8627−8635.

(4) Raghavendra, B.; Arunan, E. Unpaired and σ Bond Electrons as H, Cl, and Li Bond Acceptors: An Anomalous One-Electron Blue-Shifting Chlorine Bond. *J. Phys. Chem. A* **2007**, *111*, 9699−9706.

(5) Feller, D. Strength of the Benzene−Water Hydrogen Bond. *J. Phys. Chem. A* **1999**, *103*, 7558−7561.

(6) Li, J.; Zhang, R.-Q. Strong orbital interaction in a weak CH-π hydrogen bonding system. *Sci. Rep.* **2016**, *6*, 22304.

(7) Daolio, A.; Scilabra, P.; Terraneo, G.; Resnati, G. C(sp^3) atoms as tetrel bond donors: A crystallographic survey. *Coord. Chem. Rev.* **2020**, *413*, 213265.

(8) Bauzá, A.; Mooibroek, T. J.; Frontera, A. Tetrel-Bonding Interaction: Rediscovered Supramolecular Force? *Angew. Chem., Int. Ed.* **2013**, *52*, 12317−12321.

(9) Scheiner, S. Origins and properties of the tetrel bond. *Phys. Chem. Chem. Phys.* **2021**, *23*, 5702−5717.

(10) Echeverría, J. Alkyl groups as electron density donors in π-hole bonding. *CrystEngComm* **2017**, *19*, 6289−6296.

(11) Szczęśniak, M. M.; Chalasiński, G.; Cybulski, S. M.; Cieplak, P. Ab initio study of the potential energy surface of CH_4-H_2O. *J. Chem. Phys.* **1993**, *98*, 3078−3089.

(12) Isaev, A. N. O−H···C hydrogen bond in the methane−water complex. *Russ. J. Phys. Chem. A* **2016**, *90*, 1978−1985.

(13) Isaev, A. N. Intermolecular charge transfer as evidence for unusual O−H···C(sp^3) hydrogen bond. *Comput. Theor. Chem.* **2016**, *1090*, 180−192.

(14) Olesen, S. G.; Hammerum, S. Hydrogen Bonding to Alkanes: Computational Evidence. *J. Phys. Chem. A* **2009**, *113*, 7940−7944.

(15) Parajuli, R.; Arunan, E. X-H···C hydrogen bonds in n-alkane-HX (X = F, OH) complexes are stronger than C-H···X hydrogen bonds. *J. Chem. Sci.* **2015**, *127*, 1035−1045.

(16) Groom, C. R.; Bruno, I. J.; Lightfoot, M. P.; Ward, S. C. The Cambridge Structural Database. *Acta Crystallogr., Sect. B: Struct. Sci., Cryst. Eng. Mater.* **2016**, *72*, 171−179.

(17) Alvarez, S. A cartography of the van der Waals territories. *Dalton Trans.* **2013**, *42*, 8617−8636.

(18) Echeverría, J.; Velásquez, J. D.; Alvarez, S. Understanding the Interplay of Dispersion, Charge Transfer, and Electrostatics in Noncovalent Interactions: The Case of Bromine−Carbonyl Short Contacts. *Cryst. Growth Des.* **2020**, *20*, 7180.

(19) Velásquez, J. D.; Echeverría, J.; Alvarez, S. Effect of the Substituents on the Nature and Strength of Lone-Pair−Carbonyl Interactions in Acyl Halides. *Cryst. Growth Des.* **2019**, *19*, 6511−6518.

(20) Echeverría, J. Noncovalent Interactions in Succinic and Maleic Anhydride Derivatives. *Cryst. Growth Des.* **2018**, *18*, 506−512.

(21) Echeverría, J. Intermolecular Carbonyl···Carbonyl Interactions in Transition-Metal Complexes. *Inorg. Chem.* **2018**, *57*, 5429−5437.

(22) Lee, S. M.; Sim, K. S.; Lo, K. M. Synthesis, characterization and biological studies of diorganotin(IV) complexes with tris-[(hydroxymethyl)aminomethane] Schiff bases. *Inorg. Chim. Acta* **2015**, *429*, 195−208.

(23) Kim, K. M.; Sohn, Y. S. Reaction of Tetrahydroxo(2,2-dimethylpropane- diamine)platinum(IV) with Trimethylsilylchoride. Pentacoordinative Si···OH Interaction Labilizing the PtIV−OH Bond. *Inorg. Chem.* **1998**, *37*, 6109−6112.

(24) Lazareva, N. F.; Sterkhova, I. V.; Albanov, A. I. N-[Chloro(dimethyl)silyl]methyl-N,N′-diphenylurea: Synthesis and structure. *J. Organomet. Chem.* **2018**, *867*, 62−66.

(25) Casas, J. S.; Castaño, M. a. V.; Cifuentes, M. a. C.; Sánchez, A. n.; Sordo, J. Synthesis and structures of acetylferrocene thiosemicarbazones and their dimethylthallium(III) complexes, which have four- or five-membered chelate rings. *Polyhedron* **2002**, *21*, 1651−1660.

(26) Echeverría, J.; Aullón, G.; Alvarez, S. Intermolecular interactions in group 14 hydrides: Beyond C-H···H-C contacts. *Int. J. Quantum Chem.* **2017**, *117*, e25432.

(27) Echeverría, J.; Aullón, G.; Alvarez, S. Dihydrogen intermolecular contacts in group 13 compounds: H···H or E···H (E = B, Al, Ga) interactions? *Dalton Trans.* **2017**, *46*, 2844−2854.

(28) Echeverría, J. Abundance and Strength of M−H···H−C (M = Al, Ga, In) Dihydrogen Bonds. *Cryst. Growth Des.* **2017**, *17*, 2097−2103.

(29) Müller, J.; Ruschewitz, U.; Indris, O.; Hartwig, H.; Stahl, W. Structure of Ammonia Trimethylalane (Me_3Al-NH_3): Microwave Spectroscopy, X-ray Powder Diffraction, and ab Initio Calculations. *J. Am. Chem. Soc.* **1999**, *121*, 4647−4652.

(30) Gemünd, B.; Günther, B.; Knizek, J.; Nöth, H. N-(2,4,6-Trimethylborazinyl)-substituted Boron, Aluminum and Titanium Compounds. *Z. Naturforsch., B: J. Chem. Sci.* **2008**, *63*, 23−36.

(31) Meesakul, P.; Jaidee, W.; Richardson, C.; Andersen, R. J.; Patrick, B. O.; Willis, A. C.; Muanprasat, C.; Wang, J.; Lei, X.; Hadsadee, S.; Jungsuttiwong, S.; Pyne, S. G.; Laphookhieo, S. Styryllactones from Goniothalamus tamirensis. *Phytochemistry* **2020**, *171*, 112248.

(32) Dippel, K.; Klingebiel, U.; Kottke, T.; Pauer, F.; Sheldrick, G. M.; Stalke, D. Fluorsilyl- und Fluorboryl-substituierte Cyclotetrasilazane Synthese und Kristallstrukturen. *Z. Anorg. Allg. Chem.* **1990**, *584*, 87−104.

(33) Bader, R. F. W. *Atoms in Molecules: A Quantum Theory*; Clarendon Press: Oxford, 1990.

(34) Johnson, E. R.; Keinan, S.; Mori-Sánchez, P.; Contreras-García, J.; Cohen, A. J.; Yang, W. Revealing Noncovalent Interactions. *J. Am. Chem. Soc.* **2010**, *132*, 6498−6506.

(35) Cubero, E.; Orozco, M.; Hobza, P.; Luque, F. J. Hydrogen Bond versus Anti-Hydrogen Bond: A Comparative Analysis Based on the Electron Density Topology. *J. Phys. Chem. A* **1999**, *103*, 6394−6401.

(36) Scheiner, S.; Adhikari, U. Abilities of Different Electron Donors (D) to Engage in a P···D Noncovalent Interaction. *J. Phys. Chem. A* **2011**, *115*, 11101−11110.

(37) Kolman, V.; Marek, R.; Strelcova, Z.; Kulhanek, P.; Necas, M.; Svec, J.; Sindelar, V. Electron Density Shift in Imidazolium Derivatives upon Complexation with Cucurbit[6]uril. *Chem. - Eur. J.* **2009**, *15*, 6926−6931.

(38) Isaev, A. N. Comparative Analysis of Hydrogen, van der Waals, and Halogen Bonds in Ammonia Complexes with HCl and ClF Molecules. *Russ. J. Phys. Chem. A* **2019**, *93*, 2394−2406.

(39) Zierkiewicz, W.; Michalczyk, M.; Scheiner, S. Aerogen bonds formed between $AeOF_2$ (Ae = Kr, Xe) and diazines: comparisons between σ-hole and π-hole complexes. *Phys. Chem. Chem. Phys.* **2018**, *20*, 4676−4687.

(40) Sánchez-Sanz, G.; Trujillo, C.; Alkorta, I.; Elguero, J. Electron density shift description of non-bonding intramolecular interactions. *Comput. Theor. Chem.* **2012**, *991*, 124−133.

(41) Iribarren, I.; Sánchez-Sanz, G.; Alkorta, I.; Elguero, J.; Trujillo, C. Evaluation of Electron Density Shifts in Noncovalent Interactions. *J. Phys. Chem. A* **2021**, *125*, 4741−4749.

(42) Tang, H.-f.; Zhong, H.; Zhang, L.-l.; Gong, M.-x.; Song, S.-q.; Tian, Q.-p. Theoretical investigations into the intermolecular hydrogen-bonding interactions of N-(hydroxymethyl)acetamide dimers. *J. Mol. Model.* **2018**, *24*, 139.

(43) Bauzá, A.; Alkorta, I.; Frontera, A.; Elguero, J. On the Reliability of Pure and Hybrid DFT Methods for the Evaluation of Halogen, Chalcogen, and Pnicogen Bonds Involving Anionic and Neutral Electron Donors. *J. Chem. Theory Comput.* **2013**, *9*, 5201−5210.

(44) Kozuch, S.; Martin, J. M. L. Halogen Bonds: Benchmarks and Theoretical Analysis. *J. Chem. Theory Comput.* **2013**, *9*, 1918−1931.

https://doi.org/10.1021/acs.cgd.1c00853
Cryst. Growth Des. 2021, 21, 5961−5966

(45) Boys, S. F.; Bernardi, F. The calculation of small molecular interactions by the differences of separate total energies. Some procedures with reduced errors. *Mol. Phys.* **1970**, *19*, 553−566.
(46) Neese, F. Software update: the ORCA program system, version 4.0. *Wiley Interdiscip. Rev.: Comput. Mol. Sci.* **2018**, *8*, e1327.
(47) Frisch, M. J.; Trucks, G. W.; Schlegel, H. B.; Scuseria, G. E.; Robb, M. A.; Cheeseman, J. R.; Scalmani, G.; Barone, V.; Petersson, G. A.; Nakatsuji, H.; Li, X.; Caricato, M.; Marenich, A. V.; Bloino, J.; Janesko, B. G.; Gomperts, R.; Mennucci, B.; Hratchian, H. P.; Ortiz, J. V.; Izmaylov, A. F.; Sonnenberg, J. L.; Williams-Young, D.; Ding, F.; Lipparini, F.; Egidi, F.; Goings, J.; Peng, B.; Petrone, A.; Henderson, T.; Ranasinghe, D.; Zakrzewski, V. G.; Gao, J.; Rega, N.; Zheng, G.; Liang, W.; Hada, M.; Ehara, M.; Toyota, K.; Fukuda, R.; Hasegawa, J.; Ishida, M.; Nakajima, T.; Honda, Y.; Kitao, O.; Nakai, H.; Vreven, T.; Throssell, K.; Montgomery, J. A., Jr.; Peralta, J. E.; Ogliaro, F.; Bearpark, M. J.; Heyd, J. J.; Brothers, E. N.; Kudin, K. N.; Staroverov, V. N.; Keith, T. A.; Kobayashi, R.; Normand, J.; Raghavachari, K.; Rendell, A. P.; Burant, J. C.; Iyengar, S. S.; Tomasi, J.; Cossi, M.; Millam, J. M.; Klene, M.; Adamo, C.; Cammi, R.; Ochterski, J. W.; Martin, R. L.; Morokuma, K.; Farkas, O.; Foresman, J. B.; Fox, D. J. *Gaussian 16*, Revision B.01; Gaussian, Inc.: Wallingford CT, 2016.
(48) Dennington, R.; Keith, T.; Millam, J. *GaussView*, version 5; Semichem Inc.: Shawnee Mission, KS, 2009.
(49) Lu, T.; Chen, F. Multiwfn: A multifunctional wavefunction analyzer. *J. Comput. Chem.* **2012**, *33*, 580−592.
(50) Glendening, E. D.; Reed, A. E.; Carpenter, J. E.; Weinhold, F. *NBO*, Version 3.1, 2001.
(51) Humphrey, W.; Dalke, A.; Schulten, K. VMD: Visual molecular dynamics. *J. Mol. Graphics* **1996**, *14*, 33−38.

https://doi.org/10.1021/acs.cgd.1c00853
Cryst. Growth Des. 2021, 21, 5961−5966